

Decaying Telco Big Data with Data Postdiction

Constantinos Costa*, Andreas Charalampous*, Andreas Konstantinidis*,
Demetrios Zeinalipour-Yazti* and Mohamed F. Mokbel‡

*Department of Computer Science, University of Cyprus, 1678 Nicosia, Cyprus

‡Department of Computer Science & Engineering, University of Minnesota, Minneapolis, MN 55455, USA
{costa.c, achara28, akonstan, dzeina}@cs.ucy.ac.cy; mokbel@cs.umn.edu

Abstract—In this paper, we present a novel decaying operator for Telco Big Data (TBD), coined *TBD-DP (Data Postdiction)*. Unlike data prediction, which aims to make a statement about the future value of some tuple, our formulated *data postdiction* term, aims to make a statement about the past value of some tuple, which doesn't exist anymore as it had to be deleted to free up disk space. *TBD-DP* relies on existing Machine Learning (ML) algorithms to abstract TBD into compact models that can be stored and queried when necessary. Our proposed *TBD-DP* operator has the following two conceptual phases: (i) in an offline phase, it utilizes a LSTM-based hierarchical ML algorithm to learn a tree of models (coined *TBD-DP tree*) over time and space; (ii) in an online phase, it uses the *TBD-DP tree* to recover data within a certain accuracy. In our experimental setup, we measure the efficiency of the proposed operator using a ~ 10 GB anonymized real telco network trace and our experimental results in Tensorflow over HDFS are extremely encouraging as they show that *TBD-DP* saves an order of magnitude storage space while maintaining a high accuracy on the recovered data.

Index Terms—big data, postdiction, prediction, sampling

I. INTRODUCTION

In recent years there has been considerable interest from *telecommunication companies (telcos)* to extract concealed value from their network data. Consider for example a telco in the city of Shenzhen, China, which serves 10 million users. Such a telco is shown to produce 5TB per day [1] (i.e., thousands to millions of records every second). Huang et al. [2] break their 2.26TB per day *Telco Big Data (TBD)* down as follows: (i) *Business Supporting Systems (BSS)* data, which is generated by the internal work-flows of a telco (e.g., billing, support), accounting to a moderate of 24GB per day and; (ii) *Operation Supporting Systems (OSS)* data, which is generated by the Radio and Core equipment of a telco, accounting to 2.2TB per day and occupying over 97% of the total volume.

Effectively storing and processing TBD workflows can unlock a wide spectrum of challenges, ranging from churn prediction of subscribers [2], city localization [3], 5G network optimization / user-experience assessment [4]–[6] and road traffic mapping [7]. Even though the acquisition of TBD is instrumental in the success of the above scenarios, Telcos are reaching a point where they are collecting more data than they could possibly exploit. This has the following two implications: (i) it introduces a significant financial burden on the operator to store the collected data locally. Notice that the deep storage of data in public clouds, where economies-of-scale are available (e.g., AWS Glacier), is not an option due to

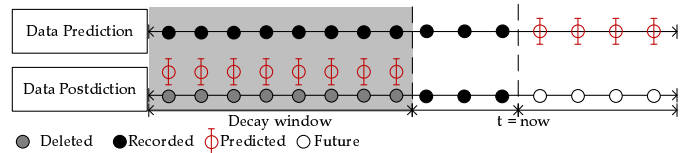


Fig. 1. **Data Prediction (top)**: aims to make a statement about the future value of some tuple. **Data Postdiction (bottom)**: aims to make a statement about the past value of some tuple, which has been deleted for efficiency reasons, using ML models.

privacy reasons; and (ii) it imposes a high computational cost for accessing and processing the collected data. For example, a petabyte Hadoop cluster, using between 125 and 250 nodes, costs ~ 1 M USD¹ and a linear scan of 1PB would require almost 15 hours. Additionally, in [8] it is shown that the amount of storage doubles every year and storage media costs decline only at a rate of less than 1/5 per year. Finally, high-availability storage mandates low-level data replication (e.g., in HDFS the default replication is 3). *Consequently, we claim that the vision of infinitely storing all IoT-generated velocity data on fast or even deep storage will gradually become too costly and impractical for processing scenarios.*

To this end, *data decaying* [9], [10] (or data rotting) has recently been suggested as a powerful concept to complement traditional data reduction techniques (e.g., sampling, histograms, sketches, compression and signal/timeseries processing tools). Data decaying refers to “*the progressive loss of detail in information as data ages with time*”. In data decaying recent data retains complete resolution, which is practical for operational scenarios that can continue to operate at full data resolution, while older data is either compacted or discarded [5], [9], [10]. Additionally, the decaying cost can be amortized over time, matching current trends in micro-batching (e.g., Apache Spark). Unfortunately, data decaying currently relies on rather straightforward methodologies, such as rotational decaying (i.e., FIFO) [9], or decaying based on specific queries [5] rather than the complete dataset itself. Our aim in this work is to expand upon these developments to provide more intelligent and generalized decaying operators.

In this paper, we present a novel decaying operator for Telco Big Data, coined *TBD-DP (Data Postdiction)* (see Figure 1).

¹April 16, 2012: Forbes Magazine, URL: <https://goo.gl/eM1uwV>

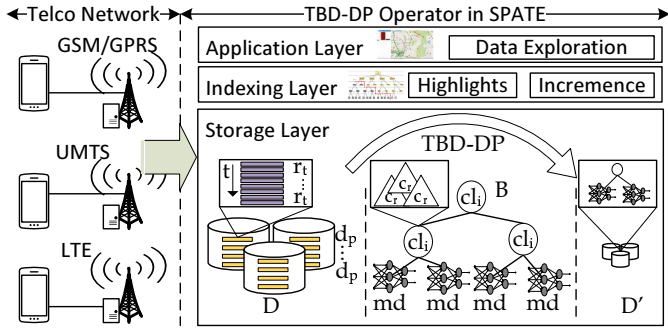


Fig. 2. System Model: The TBD-DP operator works on the storage layer of a typical TBD stack and abstracts the incoming data signals (D) into abstract models (md) that are organized in a tree data structure (B).

Unlike data prediction, which aims to make a statement about the future value of some tuple in a TBD store, data postdiction aims to make a statement about the past value of some tuple that doesn't exist anymore, as it had to be deleted to free up space. *TBD-DP* relies on existing Machine Learning (ML) algorithms to abstract TBD into compact models that can be stored and queried when necessary. Our proposed *TBD-DP* operator has the following two conceptual phases: (i) in an offline phase, it utilizes a LSTM-based hierarchical ML algorithm to learn a tree of models (coined *TBD-DP* tree) over time and space; (ii) in an online phase, it uses the *TBD-DP* tree to recover data with a certain accuracy.

To understand the operational aspects of our proposed *TBD-DP* operator, consider Figure 2, where we show how incoming telco data signals are absorbed by the TBD architecture and stored on high-availability and fast storage (i.e., D). This helps to carry out operational tasks (e.g., alerting services and visual analytics) with full data resolution. Subsequently, in the first phase of *TBD-DP*, we utilize a specialized *Recurrent Neural Network (RNN)* composed of *Long Short Term Memory (LSTM)* units, which has the ability to detect long-term correlations in activity data and the trained model has a small disk space footprint [11]. This enables *TBD-DP* to utilize minimum storage capacity of the decayed data by representing them with LSTM models on the disk media (D') and provide real-time postdictions with high accuracy in a subsequent recovery phase, which will be initiated on-demand (i.e., whenever some high-level operator requests the given data blocks).

The contributions of this work are summarized as follows:

- We propose a TBD decay operator that deploys the notion of data postdiction using off-the-shelf LSTM-based prediction models.
- We propose the DP-tree, which is a hierarchical index to organize the generated models in a data structure to enable the efficient recovery of data when necessary.
- We measure the efficiency of the proposed operator using a $\sim 10\text{GB}$ anonymized real telco network trace, showing that *TBD-DP* can be a premise for efficient TBD management in the future. We also summarize a prototype architecture and user interface we have developed for the

TABLE I
SUMMARY OF NOTATION

Notation	Description
p, d_p, D	Ingestion period, data snapshot of one p , set of all d_p s
t, r_t	Timestamp within an ingestion cycle, record at t
C, c_r, cl_i	Set of all cell towers, Cell of record r , cluster of records $i = 1, \dots, k$
md_i, MD	LSTM model of cluster cl_i , set of all models
f	Decaying factor: percentage of data to be removed

management of TBD.

II. SYSTEM MODEL AND PROBLEM FORMULATION

This section formalizes our system model, assumptions and problem. The main symbols and their respective definitions are summarized in Table I.

A typical Telco system, illustrated in Figure 2, is composed of the Telco network, which is responsible for providing telecommunication services, and a Telco data management system, such as SPATE [5], which is responsible for the efficient exploration of Telco datasets. The data arrives at the data center in batches, called henceforth data snapshots noted by d_p , in the form of horizontally segmented files with in an ingestion period p . A snapshot d_p contains multiple records r_t created at a certain timestamp t . Each record r_t consists of a predefined set of attributes including the cell id c_r that represents the spatial information inherent within the Telco network. Particularly, each cell id c_r corresponds to a cell that covers a geographical cellular area that usually spans hundreds of meters. Finally, the cells are spatially grouped into clusters $cl_i, i = 1 \dots k$ for facilitating the postdiction process by creating a model $md_i, i = 1 \dots k$ for each cl_i as this will be explained in the next section.

A. Problem Formulation

Research Goal. *Given a Telco setting, this work aims at achieving a pre-specified decaying of TBD with minimum additional storage space capacity and being able to recover the decayed data accurately and efficiently.*

The efficiency of the proposed techniques to achieve the above goal is measured by the following objectives:

Definition 2.1: Storage Capacity (S) is the total storage space required for achieving decaying of data based on a pre-specified decaying factor f .

Definition 2.2: Accuracy (NRMSE) is the percentage of the correctly recovered decayed data using a postdiction model. *NRMSE* is measured using the normalized root mean square error, which is the normalized difference between the predicted and the actual data.

III. THE TBD-DP OPERATOR

In this section, we introduce the proposed *TBD-DP* operator and discuss its two internal algorithms, namely, the *Construction* (Data model creation) and the *Recovery* (Data recreation), which capture its core functionality as illustrated in Figure 3.

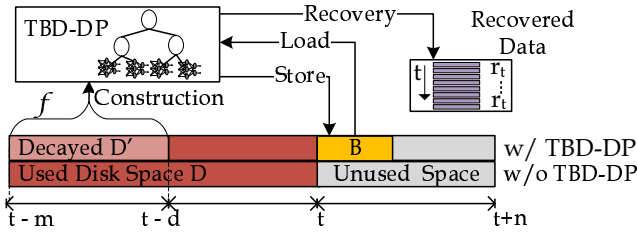


Fig. 3. TBD-DP Operator Overview.

The *Construction* algorithm can be triggered either by the user, or automatically when the total storage capacity reaches a certain level. In both cases, the data are initially clustered based on spatial characteristics and then ordered based on temporal information. Finally, postdiction models based on the LSTM machine learning approach are generated for each cluster and the real data is decayed by $f\%$. The *Recovery* algorithm utilizes the postdiction models for retrieving the decayed data by adopting a proposed DP-tree based algorithm.

A. Construction Algorithm

Algorithm 1 outlines the major steps of the construction algorithm. Initially, the decaying factor f specifies the percentage of the whole dataset D that will be decayed, and consequently the decayed subset $D' \subseteq D$ that will be utilized for generating the postdiction models. In the spatial partitioning step (Step 1 - lines 2-5), $k \leq |C|$ clusters are created by using the cell tower locations. Particularly, each cluster $cl_i, i = 1, \dots, k$ is represented by a cell tower (in cases where $k < |C|$ then the closest cell towers are merged using a kNN approach until we finally generate k clusters.) Then the *MAP* function associates all records $r_t \in D'$ with the previously created clusters by taking into consideration their cell id c_r attribute. By the end of this function execution, k clusters of cell towers with their associate records will be created. Then all records of each cluster are ordered based on their timestamp (i.e., time originally generated) by using the *ORDER* function of the temporal ordering step (Step 2 - lines 6-8). Finally, the learning step (Step 3 - lines 9-12) generates k postdiction models md_i for each cluster cl_i by using a specialized Recurrent Neural Network (RNN) known as the Long Short Term Memory (LSTM) model [12].

Specifically, the *LEARNING* function generates, for each cluster at each iteration, an LSTM model that relies on a structure called a memory cell, which is composed of four main elements: an input gate, a neuron with a self-recurrent connection (a connection to itself), a forget gate and an output gate. A memory cell is updated at every time-step by using the following parameters and equations:

- x_t is the input to the memory cell layer at time-step t
- W_i, W_f, W_C and W_o are weight matrices
- b_i, b_f, b_C and b_o are bias vectors

The forget gate layer:

$$f_t = \sigma(W_f \times [h_{t-1}, x_t] + b_f),$$

Algorithm 1 - TBD-DP Construction Algorithm

Input: Dataset D , C set of cell towers, Number of clusters k
Output: B : Set of models MD (DP-tree structure)

▷ **Step 0: Decaying Pre-processing**
1: $D' \leftarrow f$ of D ▷ Select $f\%$ of D to be decayed

▷ **Step 1: Spatial Partitioning**
2: Create $k \leq |C|$ clusters cl_i ▷ Use cell towers locations
3: **for all** $r_t \in D'$ **do**
4: $cl_i \leftarrow MAP(r_t, cl_i) | i = 1, \dots, k$ ▷ Associate records to clusters
5: **end for**

▷ **Step 2: Temporal Ordering**
6: **for** $i = 1$ to k **do**
7: $cl_i \leftarrow ORDER(cl_i)$ ▷ Sort records in clusters based on timestamp
8: **end for**

▷ **Step 3: Hierarchical Model**
9: **for** $i = 1$ to k **do**
10: $md_i \leftarrow LEARNING(cl_i)$ ▷ Create an LSTM model for each cl_i
11: Insert md_i in B
12: **end for**

decides what information are going to be thrown away from the memory cells. The input gate layer:

$$i_t = s(W_i[h_{t-1}, x_t] + b_i),$$

decides which values to be updated. The tanh layer decides what new information we are going to store in the memory cells using:

$$\tilde{C}_t = \tanh(W_C[h_{t-1}, x_t] + b_C).$$

Moreover, the update memory cells function:

$$C_t = f_t \times C_{t-1} + i_t \times \tilde{C}_t,$$

used to forget the things decided to be forgotten earlier and scale the new candidate values by a pre-specified state value.

Finally, the update hidden cells function:

$$o_t = \sigma(W_o[h_{t-1}, x_t] + b_o)$$

and a sigmoid layer that decide what parts of the cell state to output,

$$h_t = o_t * \tanh(C_t).$$

The *Construction* algorithm outputs a set of postdiction models B in a DP-tree for facilitating the recovery algorithm that follows. Here it is important to note that at the end of the *Construction* algorithm execution, the D' set of data is removed for saving storage space and it is conceptually replaced by the final B set of postdiction models, where $|B| \ll |D'|$.

Example: Consider the scenario in Figure 4 where there are 10 cell towers $\{A, \dots, J\}$. First, the *Construction* algorithm creates $k = 5$ clusters $\{cl_1, \dots, cl_5\}$ denoted with the solid line that surrounds the cell towers in Step 1 of Figure 4 (left). The *MAP* function associates the records to a cluster based on the cell id c_r (e.g., all records related to A and B are grouped into cl_1). Then, the *ORDER* function sorts the records of each cluster based on their timestamp t as shown in Step 2 of Figure 4 (center). Finally, for each cluster cl_i a model md_i

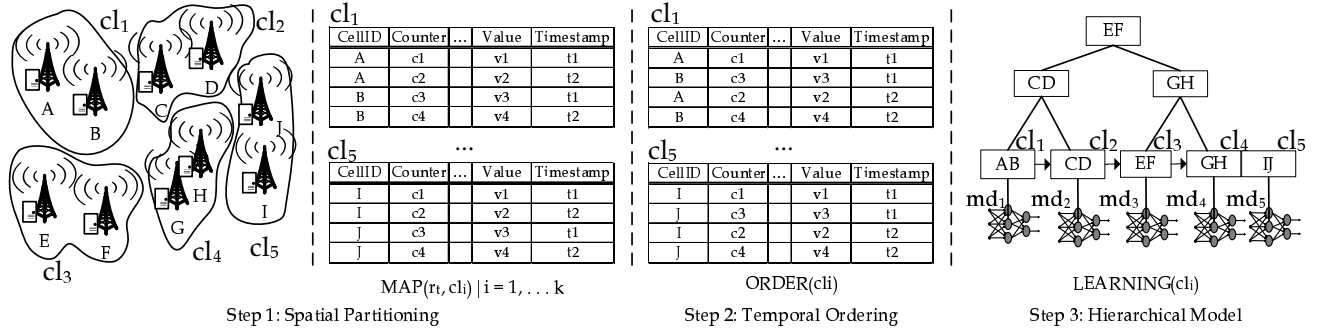


Fig. 4. The conceptual steps of the proposed *TBD-DP* construction algorithm.

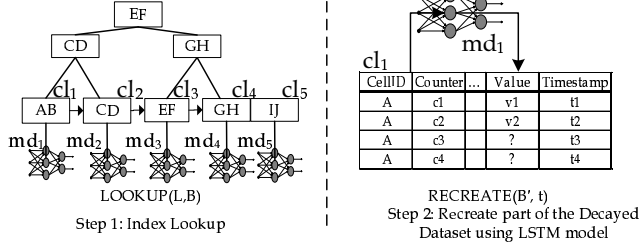


Fig. 5. The conceptual steps of the proposed *TBD-DP* recovery algorithm.

is trained and inserted into a DP-tree index using the cell ids as keys, as shown in Figure 4 (right).

B. Recovery Algorithm

Algorithm 2 outlines the *Recovery* algorithm that utilizes the DP-tree structure of postdiction models of Algorithm 1 for retrieving a selected subset from the decayed data, i.e., $pD' \subseteq D'$. For doing this the *Recovery* algorithm inputs the set of models B as well as some spatiotemporal information L and R that will specify the amount of the decayed data to be retrieved. For example, L can be a cellular tower's location or a user's location associated to a cellular tower and R can be a range of timestamps, within which a number of records were generated and stored in D' . In any case, L and R will be utilized by the DP-tree *LOOKUP* function for deciding a subset of models $B' \subseteq B$ in line 13 that will be used for creating the pD' dataset in line 15.

Example: Consider the scenario where the data of cell tower A needs to be recovered for timestamps t_1, \dots, t_4 . *LOOKUP* retrieves the LSTM model md_1 for cluster cl_1 created from all records related to cell towers A and B as shown in Step 1 of Figure 5 (left). In Step 2 of Figure 5 (right), the *Recovery* algorithm recreates the values of cell tower A for each timestamp t recovering in this way a part of the decayed data pD' using the selected LSTM model.

C. Performance Analysis

The major focus of *TBD-DP* is the efficient decaying of data and consequently the minimization of TBD storage space while maintaining a high accuracy during data recovery.

Algorithm 2 - *TBD-DP* Recovery Algorithm

Input: L : spatial input; R : temporal input; B : set of postdiction models in a DP-tree structure

Output: Partial decayed dataset pD'

```

1: procedure LOOKUP( $k, node$ ) ▷ The number of children is  $b$ .
2:   if  $node$  is a leaf then
3:     return  $node$ 
4:   end if
5:   switch  $k$  do
6:     case  $k < k_0$ 
7:       return LOOKUP( $k, p_0$ )
8:     case  $k_i \leq k < k_{i+1}$ 
9:       return LOOKUP( $k, p_{i+1}$ )
10:    case  $k_d \leq k$  ▷ Each node has at most  $d \leq b$ 
11:      return LOOKUP( $k, p_{d+1}$ )
12:  end procedure
13:  $B' \leftarrow$  LOOKUP( $L, B$ ) ▷ Select a subset of postdiction models
14: for all  $t \in R$  do
15:    $pD' =$  RECREATE( $B', t$ ) ▷ Retrieve decayed data of specific time periods.
16: end for

```

According to Definition 2.1 the total storage space S is equal to the actual data minus the decayed data based on f , plus any additional storage required by the decaying approach to achieve an optimal recreation of the decayed data. When there is no decaying $f = 0\%$ (that is the standard prediction case) then $S = |D| + |B|$, which is the size of the actual (raw) data D and the size of the set of prediction models B . In the case of *TBD-DP*, $S = |D| - |D'| + |B|$, which is the actual data size minus the size of the decayed dataset $|D'| = |D| \times f\%$ plus the size of a set of models B , where $|D| \gg |D'| + |B|$. When $f = 100\%$ then all data are decayed and the required storage space of *TBD-DP* is $S = |B|$. In the case of sampling, the storage space is equal to $S = |D| - |V|$, which is the actual data size minus a sample set $V = sampling(D', s)$ generated by sampling the decayed dataset D' with a pre-specified rate s . Note that $|D| - |D'| + |B| \ll |D| - |V|$ for a reasonable s that provides an *NRMSE* similar to *TBD-DP*.

According to Definition 2.2 the *NRMSE* measures the similarity of the decayed dataset D' and the recovered dataset pD' . Therefore, in cases where the decaying factor is $f = 0\%$, which corresponds to a low $|D'| = 0$ and no decaying is

applied then $NRMSE = 0$ and when $f = 100\%$, which corresponds to a high $|D'| = |D|$ and all data are discarded then $NRMSE \gg 0$. Moreover, it is reasonable to assume that in sampling, where a sample set V of the decayed data D' is permanently discarded with a sampling rate s then, its $NRMSE(V, D')$ will be equal to the normalized difference between the sampled and the actual data. Finally, the $NRMSE$ of the proposed $TBD-DP$ will be equal to the normalized difference between the predicted data of the LSTM model and the actual data, i.e., $NRMSE(pD', D')$.

IV. PROTOTYPE DESCRIPTION

We have developed a complete prototype architecture that integrates $TBD-DP$ as part of the TBD Awareness project². Our proposed architecture comprises of three layers (see Figure 6), namely Storage Layer, Indexing Layer and Application Layer.

The *Storage layer* passes newly arrived network snapshots through a lossless compression process storing the results on a replicated big data file system for availability and performance. This component is responsible for minimizing the required storage space with minimal overhead on the query response time. The intuition is to use compression techniques that yield high compression ratios but at the same time guarantee small decompression times. We particularly use GZIP compression that offers high compression/decompression speeds, with a high compression ratio and maximum compatibility with I/O stream libraries in a typical big data ecosystem we use. Additionally, this layer uses the $TBD-DP$ operator in order to provide the decay methods for the next layer. The storage layer is basically only responsible for the leaf pages of the $SPATE$ index described in the next layer.

The Indexing Layer uses a multi-resolution spatio-temporal index, which is incremented on the rightmost path with every new data snapshot that arrives (i.e., every 30 minutes). In addition, the component computes interesting event summaries, called “highlights”, from data stored in children nodes and stores them at the parent node. For each data exploration query, the internal node that covers the temporal window of the query is accessed, and its highlights are used to answer the query.

The Application Layer implements the querying module and the *data exploration* interfaces, which receive the data exploration queries in visual or declarative mode and use the index to combine the needed highlights and snapshots to answer the query. $SPATE$ is equipped with an easy-to-use map-based web interface layer that hides the complexity of the system through a simple and elegant web interface.

V. EXPERIMENTAL METHODOLOGY AND EVALUATION

This section presents an experimental evaluation of our proposed $TBD-DP$ operator. We start-out with the experimental methodology and setup, followed by two experiments. Particularly, in the first experiment, the performance of $TBD-DP$ is compared against two baseline approaches and two

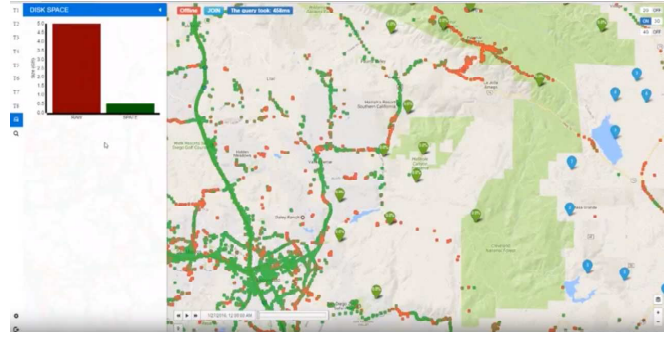


Fig. 6. $SPATE$: The decay module of $SPATE$ uses the $TBD-DP$ operator to enable the decay process and retain the high exploration functionality without consuming enormous amounts of storage.

decaying-based approaches with respect to various metrics on a set of anonymized datasets. The second experiment examines the influence of several control parameters on the performance of $TBD-DP$.

A. Methodology

This section provides details regarding the algorithms, metrics and datasets used for evaluating the performance of the proposed approach.

Testbed: Our evaluation is carried out on the DMSL VCenter IaaS datacenter, a private cloud, which encompasses 5 IBM System x3550 M3 and HP Proliant DL 360 G7 rackables featuring single socket (8 cores) or dual socket (16 cores) Intel(R) Xeon(R) CPU E5620 @ 2.40GHz, respectively. These hosts have collectively 300GB of main memory, 16TB of RAID-5 storage on an IBM 3512 and are interconnected through a Gigabit network. The datacenter is managed through a VMWare vCenter Server 5.1 that connects to the respective VMWare ESXi 5.0.0 hosts. Computing Nodes: The computing cluster, deployed over our VCenter IaaS, comprises of 4 Ubuntu 16.04 server images, each featuring 8GB of RAM with 2 virtual CPUs (@ 2.40GHz). The images utilize fast local 10K RPM RAID-5 LSI Logic SCSI disks, formatted with VMFS 5.54 (1MB block size). Each node features Hadoop v2.5.2.

We utilize measurements from a real Telco operator that comprises of 1192 real cell towers (i.e., 3660 cells of 2G, 3G and LTE networks) distributed in an area of 5,896 km². The cells are connected through a Gigabit network to a datacenter. Each cell tower keeps several UMTS/GSM network logs for the performance of the tower and forwards the information through the base station controller (BSC) or the radio network controller (RNC) to be stored. There is a CDR server that generates call detail records (CDRs) for incoming and outgoing calls in the enterprise. When a CDR is generated in the CDR server, the management server and third-party application can use SFTP to obtain the CDR from the CDR server. Then the Telco can query the CDRs for call/data information and check outgoing call/data fees with the carrier.

²TBD Awareness, <https://tbd.cs.ucy.ac.cy/>

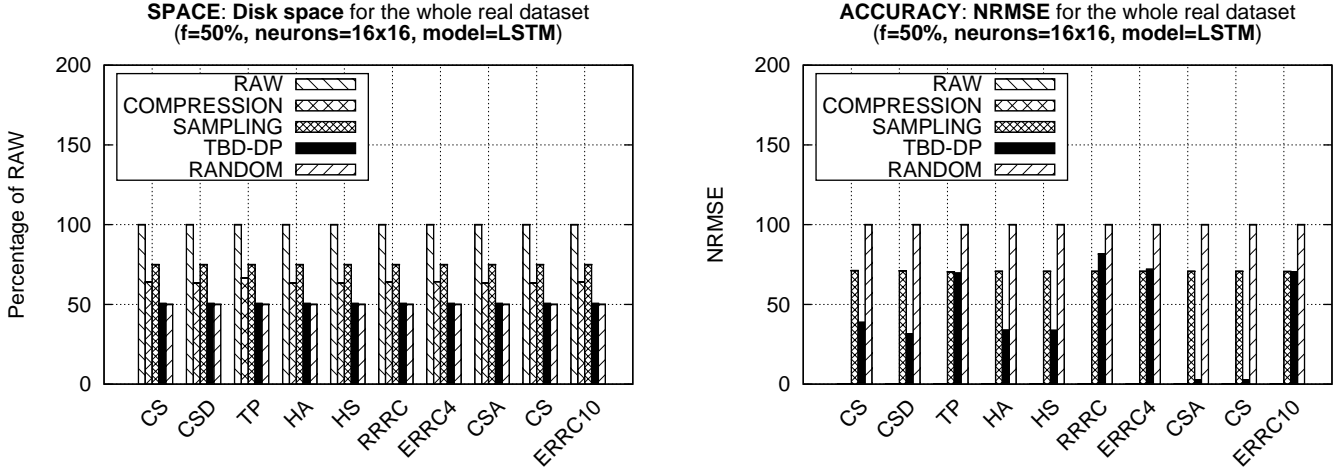


Fig. 7. Performance Evaluation: *TBD-DP* evaluation in terms of storage capacity S as a percentage to the RAW data (left) and accuracy in terms of *NRMSE* on the decayed set of data (right) in all datasets.

Algorithms: The proposed *TBD-DP* operator is compared with the following approaches:

- **RAW:** does not apply any decaying on the whole dataset.
- **COMPRESSION:** the decayed dataset (that is the subset of data selected based on the decaying factor f) is compressed with the *GZIP* library, which has been shown in [5] to offer the best balance between compression/decompression speeds, compression ratios and compatibility with I/O stream libraries in the TBD software ecosystem.
- **SAMPLING:** a consecutive sampling algorithm used for achieving a 50% sample size on the decayed dataset.
- **RANDOM:** uniformly randomly select one record from the decayed dataset.

Note that RAW and RANDOM are the baseline approaches used to demonstrate the trade-off between the storage capacity and the normalized RMSE objectives.

Datasets: We utilize an anonymized dataset of Telco traces comprising of ~ 100 M network measurements records (NMS) and 3660 cells (CELL) coming from 2G, 3G and LTE antennas. The data traffic is created from about 300K users and has a total size of ~ 10 GB. We constructed 10 realistic datasets from real TBD obtained through *SPATE* described in Section V-A based on the *Key Performance Indicators (KPIs)* [13].

- **Calls (CS):** the number of calls ended normally during snapshot d_t .
- **Call Drops (CSD):** the number of calls dropped during snapshot d_t .
- **ThroughPut (TP):** the amount of data passing through the cells during a snapshot d_t .
- **Handover Attempts (HA):** the amount of handovers into or from the cells attempted during a snapshot d_t .
- **Handovers (HS):** the number of successful handovers into or from the cells during a snapshot d_t .
- **Number of Received RRC (RRRC):** the number of received Radio Resource Control (RRC) requests for CS

Services in a Cell during a snapshot d_t .

- **Number of RRC Connection Establishment Requests (ERRC4):** the number of RRC Connection Establishment Requests with Propagation Delay of 4 during snapshot d_t .
- **Call Setup Attempts (CSA):** the amount of call setup processes attempted during snapshot d_t .
- **Call Setups (CS):** the amount of successful call setup processes during snapshot d_t .
- **RRC Connection Establishment Requests (ERRC10):** the number of RRC Connection Establishment Requests with Propagation Delay of 10-16 during snapshot d_t .

Metrics: We evaluate the performance of *TBD-DP* using the metrics defined in Section II-A in all experiments:

- **Storage Capacity (S):** measures the total space that data and index occupy throughout the distributed system in Megabytes (MB).
- **Normalized Root Mean Square Error (*NRMSE*):** measures the error of the recovered data D' using the well-known *Normalized root Mean Square Error (NRMSE)*. The objective for a technique is to obtain the lowest possible *NRMSE* value.

Parameters: In all experiments the simulation parameters were configured as follows: decay factor $f = 50\%$, ML model LSTM and number of neurons 16 x 16. The influence of each of those parameters on the proposed approach is investigated individually in Experiment 2 by fixing the rest of the parameters accordingly.

B. Experiment 1: Performance Evaluation

In the first experiment, we evaluate the performance of the proposed *TBD-DP* operator against all four algorithms and over all datasets introduced in Section V-A, with respect to space capacity (as a percentage to the RAW data) and accuracy (in terms of *NRMSE* on the decayed set of data).

Figure 7 clearly demonstrates the trade-off between the space capacity S and the *NRMSE* objectives on the results of

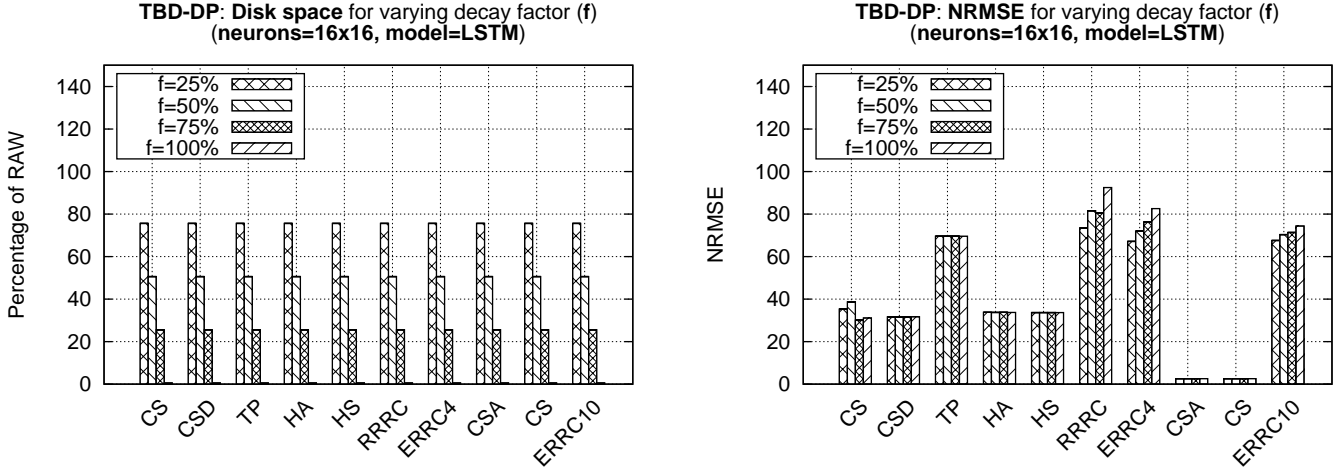


Fig. 8. Control Experiment - Decaying factor f : examining the storage capacity S and $NRMSE$ of the proposed $TBD-DP$ approach while varying f .

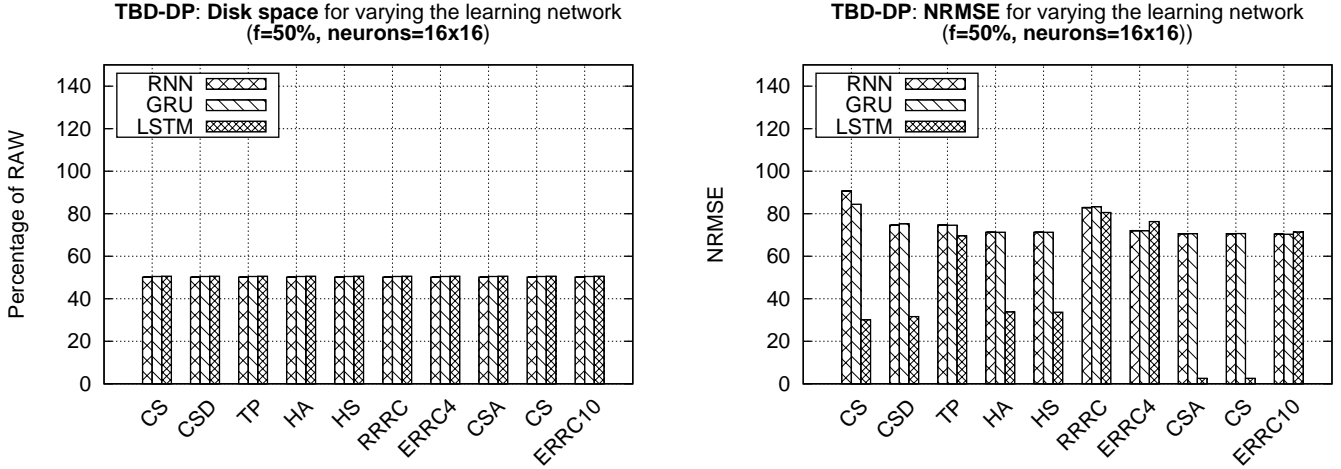


Fig. 9. Control Experiment - Learning Models: examining the storage capacity S and $NRMSE$ of the proposed $TBD-DP$ approach while combined with various ML models.

the baseline approaches, since RAW (no decaying) approach obtained the worst possible $S = 100\%$ of the whole dataset, and the lowest error $NRMSE = 0$. In contrast, the $RANDOM$ (almost all data are decayed) approach obtained the best possible $S = 50\%$ of the whole dataset and the worst $NRMSE \approx 100$ on the decayed dataset, for a decaying factor $f = 50\%$. The results of the three other approaches appear in between the results of the two baseline approaches. The proposed $TBD-DP$ operator, however, provides around 25% and 50% better space capacity S compared to $COMPRESSION$ and $SAMPLING$ approaches, respectively. This is due to the fact that the additional space required by the set of LSTM models is much less than the sample set of $SAMPLING$ and the compressed decayed dataset of $COMPRESSION$.

In terms of $NRMSE$, the $TBD-DP$ outperforms the $SAMPLING$ approach by 50%, on average, in all datasets. The $COMPRESSION$ approach provides an optimal $NRMSE = 0$, since it does not apply any prediction on the decayed data, but recovers them via decompression, when requested. The

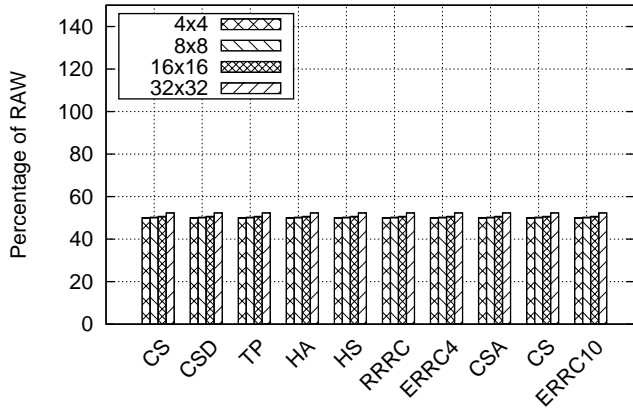
advantage of $COMPRESSION$, however, is usually achieved in the sake of more computational effort and query response time.

C. Experiment 2: Control Experiments

In Experiment 2, we examine the influence of several control parameters on the performance of the proposed $TBD-DP$ in terms of S and $NRMSE$. Specifically, we vary the decay factor (f), the ML models and the number of neurons on LSTM.

Figure 8 shows how the decaying factor f , and consequently the amount of data that will be decayed and represented by LSTM models, affect the S and $NRMSE$ of the proposed $TBD-DP$ operator. The results show that the storage capacity required by the $TBD-DP$ decreases as the decaying factor increases, which is reasonable due to the fact that the highest f is, the more data need to be decayed and therefore more disk space will be released. The accuracy of the proposed $TBD-DP$ however, is not influenced, since $NRMSE$ remains almost the

TBD-DP: Disk space for varying the number of neurons
($f=50\%$, model=LSTM)



TBD-DP: NRMSE for varying the number of neurons
($f=50\%$, model=LSTM)

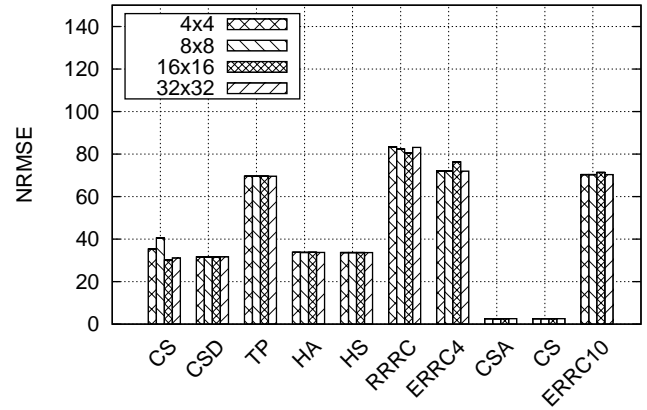


Fig. 10. Control Experiment - Number of neurons in LSTM: examining the storage capacity S and $NRMSE$ of the proposed $TBD-DP$ approach while varying the number of neurons in the LSTM.

same for all decaying factors, in most datasets. This shows the scalability and generalizability of the proposed approach, which is not influenced from the increase on the decaying dataset size. It is also important to note that the variations on the $NRMSE$ obtained by $TBD-DP$ between the datasets is mainly due to the different characteristics of each dataset.

Figure 9 examines the performance of the $TBD-DP$ operator in terms of S and $NRMSE$ when combined with three different ML models, namely, the traditional Recurrent Neural Network (RNN), the Gated Recurrent Unit (GRU) [14] and the Long Short Term Memory (LSTM) that is finally adopted by the proposed approach. The results show that $TBD-DP$ maintains a similar storage capacity for different learning models, with a slight increase (about 1%) when the LSTM model is used. In terms of $NRMSE$, however, the $TBD-DP+LSTM$ combination clearly outperforms the other two combinations providing around 75% less error, on average.

Finally, Figure 10 examines how the number of neurons of the LSTM model influences the $TBD-DP$'s performance. The results support our previous observations on the scalability and generalizability of the proposed $TBD-DP$ approach. The increase on the number of neurons slightly influences the $TBD-DP$ in terms of storage capacity, since the required space slightly increases. This is reasonable since the increase on the number of neurons results in “bigger” models that require more disk space to be stored. The additional required space, however, is almost negligible compared to the disk space needed to store the actual data before decaying. In terms of $NRMSE$, the increase on the number of neurons doesn't influence the performance of the $TBD-DP$ operator, since $NRMSE$ remains almost the same while varying this control parameter in almost all datasets.

VI. RELATED WORK

In this section, we present existing research that exploits space and time over TBD. These works are not directly comparable to $TBD-DP$ but are presented for completeness.

A. Compressing Incremental Archives

Domain-specific compression techniques are often adopted for compressing spatiotemporal climate data [15], text document collections [16], scientific simulation floating point data [17]–[21], and floating point data streams [22]. Moreover, several research studies [23]–[26] have utilized differential compression techniques for studying the tradeoff between compression ratio and decompression times for incremental archival data. None of these prior research works, however, has been proposed for dealing with data compression in Telco-specific distributed systems, since Telco datasets mostly contain generic string and integer values.

B. Telco Big Data (TBD) Research

Telco research can be roughly classified into the following three categories: (i) real-time analytics and detection; (ii) predicting user behavior; and (iii) privacy. There is also Telco research that focus on applications that Telcos can use to improve their services and revenue. Such kind of literature, however, is orthogonal to the topic of this article and will, therefore, not be presented.

Real-time Analytics and Detection: Zhang et al. [1] have developed *OceanRT* for managing large spatiotemporal data, such as Telco OSS data, running on top of cloud infrastructure. It contains a novel storage scheme that optimizes queries with joins and multi-dimensional selections. Yuan et al. [27] present *OceanST* which features (i) an efficient loading mechanism of ever-growing Telco MBB data, (ii) new spatiotemporal index structures to process exact and approximate spatiotemporal aggregate queries in order to cope with the huge volume of MBB data. Iyer et al. [4] present *CellIQ* to optimize queries such as “spatiotemporal traffic hotspots” and “handoff sequences with performance problems”. It represents the snapshots of cellular network data as graphs and leverages on the spatial and temporal locality of cellular network data.

Braun et al. [28] developed a scalable distributed system that efficiently processes mixed workloads to answer event stream and analytic queries over Telco data. Bouillet et al. [29] proposed a system on top of IBM's InfoSphere Streams middleware that analyzes 6 billion CDRs per day in real-time. Abbasoğlu et al. [30] present a system for maintaining call profiles of customers in a streaming setting by applying distributed stream processing.

C. Big Data Storage

Big data storage technologies have recently evolved in order to accommodate the huge big data load generated by IoT and smart devices. Typically, big data storage systems are distributed with shared-nothing architectures, such as the Hadoop Distributed File System (HDFS). Additionally, NoSQL databases introduce key-value stores (e.g. DynamoDB, Cassandra), column stores (e.g., HBase), document stores (e.g., Couchbase, CouchDB, MongoDB) and graph databases (e.g., Neo4j). Hive and Impala are new big data query platforms build on top of HDFS or HBase providing an SQL-like query language. Particularly, novel distributed file systems, such as OctopusFS, manage the data using heterogeneous storage media [31] but none of these systems deploys data decaying principles like the propositions in this work.

D. Data Synopsis

Sampling refers to the process of randomly selecting a subset of data elements from a relatively large dataset. Sophisticated techniques, such as Bernoulli and Poisson sampling, choose data elements using probabilities and statistics. Chaudhuri et al. [32] proposed stratified where the probability of the selection is biased. In order to encounter the big data sampling issue Zeng et al. [33] implemented G-OLA, which is a model that generalize the OLA in order to support general OLAP queries utilizing delta maintenance algorithms. Particularly, BlinkDB [34] allows users to choose the error bounds and the response time of query using dynamic sampling algorithms. SciBORQ [35] is a framework that allows the user to choose the quality of the query result based on multiple interesting data samples called impressions.

Several works have adapted the sampling processes to create synopsis of data in order to achieve low response time for ad-hoc queries [35]. Moreover, Zeng et al. [33] proposed a novel online aggregation model to support OLAP queries using delta maintenance techniques. Data sketches, which are stores in memory, require little modifications to alter the sketches on an insertion or deletion of a row [36] that makes them very flexible. Additionally, Wei et al. proposed persistent sketches that can answer queries at any prior time [37] and have the ability to merge in order to answer a generalize query [38].

E. Learning

Telcos focus on user activity predictions for optimizing their network, in terms of minimizing deployment cost and energy consumption [39]. Huang et al. [2] showed how ML algorithms can be applied over TBD to predict Telco customer

churn. Moreover, Kasiran et al. [40] also predicted the Telco customers churn using two new variations of Recurrent Neural Network (RNN), namely Elman and Jordan. Luo et al. [6] proposed a framework to predict user behavior involving more than one million Telco users. Their framework was using documents containing a collection of changing spatiotemporal “words” that described the user and his/her behavior. By extracting the users space-time access records from MBB dataset, the ML model was able to learn user-specific compact topic features achieving high user activity level prediction. Additionally, Krishna et al. [11] used an LSTM network to detect long term correlations in human activity data. The authors showed that LSTM is performing significantly better compared to traditional approaches based on sequence mining or hidden Markov models.

VII. CONCLUSIONS

This paper presents the *TBD-DP* (Data-Postdiction) decay operator that aims at minimizing TBD storage capacity by using data decaying, but also keeping the accuracy of the query results high, by using data postdiction. Particularly, *TBD-DP* initially clusters all anonymous Telco data by using spatio-temporal information of real Telco users and then utilizes a LSTM-based ML algorithm and a hierarchical index approach to achieve decaying of TBD without sacrificing the accuracy of the results. In our experiment setup, we measure the efficiency of the proposed operator using a ~ 10 GB anonymized real Telco network trace and our experimental results show that *TBD-DP* saves an order of magnitude storage space while maintaining a high accuracy during data recovery.

REFERENCES

- [1] S. Zhang, Y. Yang, W. Fan, L. Lan, and M. Yuan, “Oceanrt: Real-time analytics over large temporal data,” in *Proceedings of the 2014 ACM SIGMOD International Conference on Management of Data*, ser. SIGMOD '14. New York, NY, USA: ACM, 2014, pp. 1099–1102.
- [2] Y. Huang, F. Zhu, M. Yuan, K. Deng, Y. Li, B. Ni, W. Dai, Q. Yang, and J. Zeng, “Telco churn prediction with big data,” in *Proceedings of the 2015 ACM SIGMOD International Conference on Management of Data*, ser. SIGMOD. New York, NY, USA: ACM, 2015, pp. 607–618.
- [3] F. Zhu, C. Luo, M. Yuan, Y. Zhu, Z. Zhang, T. Gu, K. Deng, W. Rao, and J. Zeng, “City-scale localization with telco big data,” in *Proceedings of the 25th ACM International Conference on Information and Knowledge Management*, ser. CIKM. New York, NY, USA: ACM, 2016, pp. 439–448.
- [4] A. P. Iyer, L. E. Li, and I. Stoica, “Celliq: Real-time cellular network analytics at scale,” in *Proceedings of the 12th USENIX Conference on Networked Systems Design and Implementation*, ser. NSDI'15. Berkeley, CA, USA: USENIX Association, 2015, pp. 309–322.
- [5] C. Costa, G. Chatzimilioudis, D. Zeinalipour-Yazti, and M. F. Mokbel, “Efficient exploration of telco big data with compression and decaying,” in *2017 IEEE 33rd International Conference on Data Engineering (ICDE)*, April 2017, pp. 1332–1343.
- [6] C. Luo, J. Zeng, M. Yuan, W. Dai, and Q. Yang, “Telco user activity level prediction with massive mobile broadband data,” *ACM Trans. Intell. Syst. Technol.*, vol. 7, no. 4, pp. 63:1–63:30, May 2016.
- [7] C. Costa, G. Chatzimilioudis, D. Zeinalipour-Yazti, and M. F. Mokbel, “Towards real-time road traffic analytics using telco big data,” in *Proceedings of the International Workshop on Real-Time Business Intelligence and Analytics, BIRTE, Munich, Germany, August 28, 2017*, 2017, pp. 5:1–5:5. [Online]. Available: <http://doi.acm.org/10.1145/3129292.3129296>

- [8] C. LaChapelle, "The cost of data storage and management: where is the it headed in 2016?" 2016. [Online]. Available: <http://www.datacenterjournal.com/cost-data-storage-management-headed-2016/>
- [9] M. L. Kersten and L. Sidirouros, "A database system with amnesia." in *CIDR*, 2017.
- [10] M. L. Kersten, "Big data space fungus," in *CIDR 2015, Seventh Biennial Conference on Innovative Data Systems Research, Asilomar, CA, USA, January 4-7, 2015, Online Proceedings*, 2015.
- [11] K. Krishna, D. Jain, S. V. Mehta, and S. Choudhary, "An lstm based system for prediction of human activities with durations," *Proc. ACM Interact. Mob. Wearable Ubiquitous Technol.*, vol. 1, no. 4, pp. 147:1–147:31, Jan. 2018. [Online]. Available: <http://doi.acm.org/10.1145/3161201>
- [12] S. Hochreiter and J. Schmidhuber, "Long short-term memory," *Neural Comput.*, vol. 9, no. 8, pp. 1735–1780, Nov. 1997. [Online]. Available: <http://dx.doi.org/10.1162/neco.1997.9.8.1735>
- [13] J. Laiho, A. Wacker, and T. Novosad, *Radio Network Planning and Optimisation for UMTS*. John Wiley & Sons, 2006.
- [14] R. Dey and F. M. Salemt, "Gate-variants of gated recurrent unit (gru) neural networks," in *2017 IEEE 60th International Midwest Symposium on Circuits and Systems (MWSCAS)*, Aug 2017, pp. 1597–1600.
- [15] T. Bicer, J. Yin, D. Chiu, G. Agrawal, and K. Schuchardt, "Integrating online compression to accelerate large-scale data analytics applications," in *Parallel & Distributed Processing (IPDPS), 2013 IEEE 27th International Symposium on*. IEEE, 2013, pp. 1205–1216.
- [16] H. Yan, S. Ding, and T. Suel, "Inverted index compression and query processing with optimized document ordering," in *Proceedings of the 18th international conference on World wide web*. ACM, 2009, pp. 401–410.
- [17] S. Lakshminarasimhan, N. Shah, S. Ethier, S. Klasky, R. Latham, R. Ross, and N. F. Samatova, "Compressing the incompressible with isabela: In-situ reduction of spatio-temporal data," in *European Conference on Parallel Processing*. Springer, 2011, pp. 366–379.
- [18] E. R. Schendel, Y. Jin, N. Shah, J. Chen, C.-S. Chang, S.-H. Ku, S. Ethier, S. Klasky, R. Latham, R. Ross *et al.*, "Isobar preconditioner for effective and high-throughput lossless data compression," in *2012 IEEE 28th International Conference on Data Engineering*. IEEE, 2012, pp. 138–149.
- [19] J. Jenkins, I. Arkatkar, S. Lakshminarasimhan, D. A. Boyuka II, E. R. Schendel, N. Shah, S. Ethier, C.-S. Chang, J. Chen, H. Kolla *et al.*, "Alacrity: Analytics-driven lossless data compression for rapid in-situ indexing, storing, and querying," in *Transactions on Large-Scale Data and Knowledge-Centered Systems X*. Springer, 2013, pp. 95–114.
- [20] E. Soroush and M. Balazinska, "Time travel in a scientific array database," in *Data Engineering (ICDE), 2013 IEEE 29th International Conference on*. IEEE, 2013, pp. 98–109.
- [21] S. Bhattacharjee, A. Deshpande, and A. Sussman, "Pstore: An efficient storage framework for managing scientific data," in *Proceedings of the 26th International Conference on Scientific and Statistical Database Management*, ser. SSDBM '14. New York, NY, USA: ACM, 2014, pp. 25:1–25:12. [Online]. Available: <http://doi.acm.org/10.1145/2618243.2618268>
- [22] M. Burtscher and P. Ratanaworabhan, "Fpc: A high-speed compressor for double-precision floating-point data," *IEEE Transactions on Computers*, vol. 58, no. 1, pp. 18–31, 2009.
- [23] F. Douglis and A. Iyengar, "Application-specific delta-encoding via resemblance detection," in *USENIX Annual Technical Conference, General Track*, 2003, pp. 113–126.
- [24] D. Bhagwat, K. Eshghi, D. D. Long, and M. Lillibridge, "Extreme binning: Scalable, parallel deduplication for chunk-based file backup," in *2009 IEEE International Symposium on Modeling, Analysis & Simulation of Computer and Telecommunication Systems*. IEEE, 2009, pp. 1–9.
- [25] L. L. You, K. T. Pollack, D. D. Long, and K. Gopinath, "Presidio: a framework for efficient archival data storage," *ACM Transactions on Storage (TOS)*, vol. 7, no. 2, p. 6, 2011.
- [26] S. Bhattacharjee, A. Chavan, S. Huang, A. Deshpande, and A. Parameswaran, "Principles of dataset versioning: Exploring the recreation/storage tradeoff," *Proceedings of the VLDB Endowment*, vol. 8, no. 12, pp. 1346–1357, 2015.
- [27] M. Yuan, K. Deng, J. Zeng, Y. Li, B. Ni, X. He, F. Wang, W. Dai, and Q. Yang, "Oceanst: A distributed analytic system for large-scale spatiotemporal mobile broadband data," *Proc. VLDB Endow.*, vol. 7, no. 13, pp. 1561–1564, Aug. 2014.
- [28] L. Braun, T. Etter, G. Gasparis, M. Kaufmann, D. Kossmann, D. Widmer, A. Avitzur, A. Iliopoulos, E. Levy, and N. Liang, "Analytics in motion: High performance event-processing and real-time analytics in the same database," in *Proceedings of the 2015 ACM SIGMOD International Conference on Management of Data*, ser. SIGMOD '15. New York, NY, USA: ACM, 2015, pp. 251–264.
- [29] E. Bouillet, R. Kothari, V. Kumar, L. Mignet, S. Nathan, A. Ranganathan, D. S. Turaga, O. Udrea, and O. Verscheure, "Processing 6 billion cdrs/day: From research to production (experience report)," in *Proceedings of the 6th ACM International Conference on Distributed Event-Based Systems*, ser. DEBS '12. New York, NY, USA: ACM, 2012, pp. 264–267.
- [30] M. A. Abbasoğlu, B. Gedik, and H. Ferhatosmanoğlu, "Aggregate profile clustering for telco analytics," *Proc. VLDB Endow.*, vol. 6, no. 12, pp. 1234–1237, Aug. 2013.
- [31] E. Kakoulli and H. Herodotou, "Octopusfs: A distributed file system with tiered storage management," in *Proceedings of the 2017 ACM International Conference on Management of Data*, ser. SIGMOD '17. New York, NY, USA: ACM, 2017, pp. 65–78. [Online]. Available: <http://doi.acm.org/10.1145/3035918.3064023>
- [32] S. Chaudhuri, G. Das, and V. Narasayya, "Optimized stratified sampling for approximate query processing," *ACM Trans. Database Syst.*, vol. 32, no. 2, Jun. 2007. [Online]. Available: <http://doi.acm.org/10.1145/1242524.1242526>
- [33] K. Zeng, S. Agarwal, A. Dave, M. Armbrust, and I. Stoica, "G-ola: Generalized on-line aggregation for interactive analysis on big data," in *Proceedings of the 2015 ACM SIGMOD International Conference on Management of Data*, ser. SIGMOD '15. New York, NY, USA: ACM, 2015, pp. 913–918. [Online]. Available: <http://doi.acm.org/10.1145/2723372.2735381>
- [34] S. Agarwal, B. Mozafari, A. Panda, H. Milner, S. Madden, and I. Stoica, "Blinkdb: Queries with bounded errors and bounded response times on very large data," in *Proceedings of the 8th ACM European Conference on Computer Systems*, ser. EuroSys '13. New York, NY, USA: ACM, 2013, pp. 29–42. [Online]. Available: <http://doi.acm.org/10.1145/2465351.2465355>
- [35] L. Sidirouros, Martin, and P. Boncz, "Sciborq: Scientific data management with bounds on runtime and quality," in *In Proc. of the Intl Conf. on Innovative Data Systems Research (CIDR)*, 2011, pp. 296–301.
- [36] G. Cormode, M. Garofalakis, P. J. Haas, and C. Jermaine, "Synopses for massive data: Samples, histograms, wavelets, sketches," *Found. Trends databases*, vol. 4, no. 1–3, pp. 1–294, Jan. 2012. [Online]. Available: <http://dx.doi.org/10.1561/19000000004>
- [37] Z. Wei, G. Luo, K. Yi, X. Du, and J.-R. Wen, "Persistent data sketching," in *Proceedings of the 2015 ACM SIGMOD International Conference on Management of Data*, ser. SIGMOD '15. New York, NY, USA: ACM, 2015, pp. 795–810. [Online]. Available: <http://doi.acm.org/10.1145/2723372.2749443>
- [38] P. K. Agarwal, G. Cormode, Z. Huang, J. Phillips, Z. Wei, and K. Yi, "Mergeable summaries," in *Proceedings of the 31st ACM SIGMOD-SIGACT-SIGAI Symposium on Principles of Database Systems*, ser. PODS '12. New York, NY, USA: ACM, 2012, pp. 23–34. [Online]. Available: <http://doi.acm.org/10.1145/2213556.2213562>
- [39] C. Luo, J. Zeng, M. Yuan, W. Dai, and Q. Yang, "Telco user activity level prediction with massive mobile broadband data," *ACM Trans. Intell. Syst. Technol.*, vol. 7, no. 4, pp. 63:1–63:30, May 2016. [Online]. Available: <http://doi.acm.org/10.1145/2856057>
- [40] Z. Kasiran, Z. Ibrahim, and M. S. M. Ribuan, "Mobile phone customers churn prediction using elman and jordan recurrent neural network," in *2012 7th International Conference on Computing and Convergence Technology (ICCT)*, Dec 2012, pp. 673–678.